

# The effect of rotary inertia of added masses on vibrations of empty and fluid-filled circular cylindrical shells

M. Amabili\*, R. Garziera, S. Carra

*Dipartimento di Ingegneria Industriale, Università di Parma, Parco Area delle Scienze 181/A, Parma I-43100, Italy*

Received 15 May 2005; accepted 28 July 2005

---

## Abstract

This paper completes a study of Amabili and Garziera [2000, Vibrations of circular cylindrical shells with nonuniform constraints, elastic bed and added mass; Part I: empty and fluid-filled shells. *J. Fluids Struct.* 14, 669–690; 2002a, Vibrations of circular cylindrical shells with nonuniform constraints, elastic bed and added mass; Part II: shells containing or immersed in axial flow. *J. Fluids Struct.* 16, 31–51; 2002b, Vibrations of circular cylindrical shells with nonuniform constraints, elastic bed and added mass; Part III: steady viscous effects on shells conveying fluid. *J. Fluids Struct.* 16, 795–809] by adding the effect of rotary inertia of added masses to the DIVA code, based on the Rayleigh–Ritz method and developed to study free vibrations of circular cylindrical shells with nonuniform boundary conditions, added masses, partial elastic bed, initial pre-stress, conveying flow or immersed in axial flow. The effect of rotary inertia has also been evaluated by commercial FEM software and experiments in order to validate the DIVA code. Calculations and experiments show that the effect of rotary inertia of added masses is generally negligible, except for additional local modes; this is in contrast with what has been found for thin plates, due to the geometric stiffness of the circular cylindrical shell.

© 2005 Elsevier Ltd. All rights reserved.

---

## 1. Introduction

The effect of lumped masses on vibrations of circular cylindrical shells has been studied by many authors in the past for the important engineering applications involved; see, e.g., Leissa (1973), Soedel (1993), Amabili (1996), Amabili and Garziera (2000). In the present study, the additional effect of rotary inertia of added masses is considered, and this effect has been added to the computer program DIVA (Amabili and Garziera, 2000, 2002a, b), previously developed by the authors, in order to study free vibrations of circular cylindrical shells with nonuniform boundary conditions, conveying or immersed in flowing fluids, and subjected to pre-stress and nonuniform elastic bed.

---

\*Corresponding author. Tel.: +39 0521 905896; fax: +39 0521 905705.

E-mail address: [marco@me.unipr.it](mailto:marco@me.unipr.it) (M. Amabili).

URL: <http://me.unipr.it/mam/amabili/amabilif.html>.

## 2. Theoretical approach of DIVA code

A cylindrical coordinate system (O;  $x, r, \theta$ ) is introduced, with the origin O at the centre of the shell edge. The circular cylindrical shell has radius  $R$ , length  $L$  and uniform thickness  $h$ , and the displacement of a point on the mean surface in the axial, angular and radial directions is indicated by  $u, v$  and  $w$ , respectively. The mode shapes of the shell are expanded by using a base involving all the natural modes of the simply supported shell vibrating in vacuo. The boundary conditions of the simply supported shell are  $N_x = M_x = v = w = 0$  for  $x = 0$  and  $x = L$ , where  $N_x$  is the axial force and  $M_x$  is the bending moment per unit length. In particular, a symmetric system with respect to the angular coordinate  $\theta = 0$  is assumed. Therefore, symmetric and antisymmetric modes with respect to this axis will be considered. The symmetric modes are expanded as

$$\begin{Bmatrix} u \\ v \\ w \end{Bmatrix}_S = \sum_{n=0}^{\infty} \sum_{m=1}^{\infty} \sum_{j=1}^3 a_{nmj} \begin{Bmatrix} A_{nmj} \cos(n\theta) \cos(m\pi x/L) \\ B_{nmj} \sin(n\theta) \sin(m\pi x/L) \\ \cos(n\theta) \sin(m\pi x/L) \end{Bmatrix}, \quad (1)$$

where  $a_{nmj}$  are the unknown coefficients involved in the mode expansion,  $A_{nmj}$  and  $B_{nmj}$  are the mode shape coefficients (note that normalization of the radial displacement to 1 gives a very high value, theoretically  $\infty$ , to  $B_{nmj}$  for the axisymmetric mode ( $n = 0$ ) with prevalent angular displacement; in the numerical implementation, it is sufficient to use a large value),  $n, m$  and  $j$  indicate the number of circumferential waves, the number of axial half-waves and the mode number, respectively. In particular, the mode number  $j = 1, 2, 3$  denotes modes with prevalent radial, angular and axial displacements, respectively. In fact, it is well-known (Leissa, 1973) that the frequency equation of a simply supported shell is given by the following bi-cubic equation:

$$\Omega_{nmj}^6 - K_2 \Omega_{nmj}^4 + K_1 \Omega_{nmj}^2 - K_0 = 0, \quad (2)$$

which has three roots  $\Omega_{nmj}$  for any given values of  $n$  and  $m$ ; these roots correspond to  $j = 1, 2, 3$ . The coefficients  $K_0, K_1$  and  $K_2$  are given, e.g., in Amabili and Garziera (2000) for the Flügge theory of shells, and depend on the values of  $n$  and  $m$ . In Eq. (2),  $\Omega_{nmj}$  is the frequency parameter, defined as

$$\Omega_{nmj}^2 = \omega_{nmj}^2 R^2 \rho_S (1 - \nu^2) / E, \quad (3)$$

where  $\omega_{nmj}$  is the corresponding circular frequency,  $\rho_S$  is the shell mass density,  $E$  is Young's modulus and  $\nu$  is the Poisson ratio. The mode shape coefficients  $A_{nmj}$  and  $B_{nmj}$  are computed by a linear system that is reported, e.g., in Amabili and Garziera (2000) for the Flügge theory of shells. The antisymmetric modes with respect to  $\theta = 0$  are expanded as

$$\begin{Bmatrix} u \\ v \\ w \end{Bmatrix}_A = \sum_{n=1}^{\infty} \sum_{m=1}^{\infty} \sum_{j=1}^3 b_{nmj} \begin{Bmatrix} A_{nmj} \sin(n\theta) \cos(m\pi x/L) \\ B_{nmj} \cos(n\theta) \sin(m\pi x/L) \\ \sin(n\theta) \sin(m\pi x/L) \end{Bmatrix}. \quad (4)$$

In the case where the system loses its symmetry with respect to  $\theta = 0$ , the following mode expansion must be considered:

$$\begin{Bmatrix} u \\ v \\ w \end{Bmatrix} = \begin{Bmatrix} u \\ v \\ w \end{Bmatrix}_S + \begin{Bmatrix} u \\ v \\ w \end{Bmatrix}_A. \quad (5)$$

The reference kinetic energy  $T_S^*$  of the shell, in the general case of expansion (5), is given by

$$\begin{aligned} T_S^* &= \frac{1}{2} \rho_S h \int_0^{2\pi} \int_0^L (u^2 + v^2 + w^2) dx R d\theta \\ &= \frac{1}{2} \rho_S h R \pi L \left[ \sum_{m=1}^{\infty} \sum_{j=1}^3 a_{0mj}^2 (1 + A_{0mj}^2 + B_{0mj}^2) + \frac{1}{2} \sum_{n=1}^{\infty} \sum_{m=1}^{\infty} \sum_{j=1}^3 (a_{nmj}^2 + b_{nmj}^2) (1 + A_{nmj}^2 + B_{nmj}^2) \right]. \end{aligned} \quad (6)$$

The use of admissible functions, that are the natural modes of a less-constrained problem, allows an interesting simplification, as observed by Amabili and Garziera (1999). In fact, the maximum potential energy  $V_S$  of the shell can be obtained as the multiplication of the reference kinetic energy of a natural mode in the less-constrained problem by the corresponding eigenvalue  $\omega_{nmj}^2$  (the squared circular frequency) of the shell and by the coefficients  $a_{nmj}$  or  $b_{nmj}$ , and

then adding all the products. The result is

$$V_S = \frac{1}{2} \rho_S h R \pi L \left[ \sum_{m=1}^{\infty} \sum_{j=1}^3 a_{0mj}^2 \omega_{0mj}^2 (1 + A_{0mj}^2 + B_{0mj}^2) + \frac{1}{2} \sum_{n=1}^{\infty} \sum_{m=1}^{\infty} \sum_{j=1}^3 \omega_{nmj}^2 (a_{nmj}^2 + b_{nmj}^2) (1 + A_{nmj}^2 + B_{nmj}^2) \right]. \quad (7)$$

In Eq. (7), the orthogonality of the eigenfunctions of the less-constrained problem has been used.

The maximum potential energy  $V_{\tilde{k}}$  stored by the elastic distributed springs, which simulate the flexible axial translational constraint at  $x = 0, L$ , is given by

$$V_{\tilde{k}} = \frac{1}{2} \int_0^{2\pi} \tilde{k}(\theta) u^2(0, \theta) R d\theta + \frac{1}{2} \int_0^{2\pi} \tilde{k}(\theta) u^2(L, \theta) R d\theta. \quad (8)$$

In Eq. (8),  $\tilde{k}(\theta)$  is the nonuniform spring stiffness (N/m<sup>2</sup>) that is assumed to be the same at  $x = 0$  and  $x = L$ . For simplicity,  $\tilde{k}(\theta)$  is assumed to be symmetric with respect to  $\theta = 0$ , and it can be expanded into the following cosine series:

$$\tilde{k}(\theta) = \sum_{k=0}^{\infty} \tilde{k}_k \cos(k\theta). \quad (9)$$

From now on, the system is assumed to be symmetric with respect to  $\theta = 0$ . This hypothesis simplifies the calculations without loss of generality and can easily be removed.

The maximum potential energy  $V_c$  stored by the elastic distributed rotational springs, that simulate the flexible rotational constraint at  $x = 0, L$ , is given by

$$V_c = \frac{1}{2} \int_0^{2\pi} c(\theta) \left[ \frac{\partial w}{\partial x}(0, \theta) \right]^2 R d\theta + \frac{1}{2} \int_0^{2\pi} c(\theta) \left[ \frac{\partial w}{\partial x}(L, \theta) \right]^2 R d\theta. \quad (10)$$

In Eq. (10),  $c(\theta)$  is the nonuniform rotational spring stiffness (N) that is assumed to be the same at  $x = 0$  and  $x = L$ . Similarly to  $\tilde{k}(\theta)$ ,  $c(\theta)$  is assumed to be symmetric with respect to  $\theta = 0$ ; it can be expanded into the following cosine series:

$$c(\theta) = \sum_{k=0}^{\infty} c_k \cos(k\theta). \quad (11)$$

It is interesting to note that a fully clamped shell is obtained by setting a uniform and very high value to the stiffnesses of the translational and rotational springs  $\tilde{k}$  and  $c$ . The values of the spring stiffnesses simulating a clamped shell can be obtained by trial and error or by evaluating the edge stiffness of the shell. In fact, it was found that the natural frequencies of the system converge asymptotically to those of a clamped shell when  $\tilde{k}$  and  $c$  become very large.

A system of  $M$  lumped masses  $M_l$  (kg) at  $x = x_l^*$ ,  $\theta = \theta_l^*$  is considered. The reference translational kinetic energy of the added mass is given by

$$T_M^* = \frac{1}{2} \sum_{l=1}^M M_l [u^2(x_l^*, \theta_l^*) + v^2(x_l^*, \theta_l^*) + w^2(x_l^*, \theta_l^*)]. \quad (12)$$

As done for the boundary conditions, a symmetric distribution of added masses with respect to  $\theta = 0$  is assumed. For symmetric modes, introducing Eq. (1) into Eq. (12) one obtains

$$T_M^* = \frac{1}{2} \sum_{l=1}^M M_l \sum_{n,s=0}^{\infty} \sum_{m,i=1}^3 \sum_{j=1}^3 a_{nmj} a_{sij} \left\{ \cos(n\theta_l^*) \cos(s\theta_l^*) [\sin(m\pi x_l^*/L) \sin(i\pi x_l^*/L) + A_{nmj} A_{sij} \cos(m\pi x_l^*/L) \cos(i\pi x_l^*/L)] + B_{nmj} B_{sij} \sin(n\theta_l^*) \sin(s\theta_l^*) \sin(m\pi x_l^*/L) \sin(i\pi x_l^*/L) \right\}. \quad (13)$$

For antisymmetric modes one obtains

$$T_M^* = \frac{1}{2} \sum_{l=1}^M M_l \sum_{n,s=1}^{\infty} \sum_{m,i=1}^3 \sum_{j=1}^3 b_{nmj} b_{sij} \left\{ \sin(n\theta_l^*) \sin(s\theta_l^*) [\sin(m\pi x_l^*/L) \sin(i\pi x_l^*/L) + A_{nmj} A_{sij} \cos(m\pi x_l^*/L) \cos(i\pi x_l^*/L)] + B_{nmj} B_{sij} \cos(n\theta_l^*) \cos(s\theta_l^*) \sin(m\pi x_l^*/L) \sin(i\pi x_l^*/L) \right\}. \quad (14)$$

The reference rotary kinetic energy of the added masses is given by

$$T_{MR}^* = \frac{1}{2} \sum_{l=1}^M \left\{ J_{\theta,l} \left[ \frac{\partial w}{\partial x} (x_l^*, \theta_l^*) \right]^2 + J_{x,l} \left[ \frac{\partial w}{R \partial \theta} (x_l^*, \theta_l^*) \right]^2 \right\}, \quad (15)$$

where  $J_{x,l}$  and  $J_{\theta,l}$  are the moment of inertia of the mass  $l$  with respect to an axis parallel to  $x$  and to  $v$ , respectively, passing by the mean shell surface at mass location  $x = x_l^*$ ,  $\theta = \theta_l^*$ . For symmetric modes, introducing Eq. (1) into Eq. (15) one obtains

$$T_{MR}^* = \frac{1}{2} \sum_{l=1}^M \sum_{n,s=0}^{\infty} \sum_{m,i=1}^3 \sum_{j,\tilde{j}=1}^3 a_{nmj} a_{sij} \left\{ J_{\theta,l} \frac{m\pi}{L} \frac{i\pi}{L} \cos(n\theta_l^*) \cos(s\theta_l^*) \cos(m\pi x_l^*/L) \cos(i\pi x_l^*/L) \right. \\ \left. + J_{x,l} \frac{n}{R} \frac{s}{R} \sin(n\theta_l^*) \sin(s\theta_l^*) \sin(m\pi x_l^*/L) \sin(i\pi x_l^*/L) \right\}. \quad (16)$$

For antisymmetric modes one obtains

$$T_{MR}^* = \frac{1}{2} \sum_{l=1}^M \sum_{n,s=1}^{\infty} \sum_{m,i=1}^3 \sum_{j,\tilde{j}=1}^3 b_{nmj} b_{sij} \left\{ J_{\theta,l} \frac{m\pi}{L} \frac{i\pi}{L} \sin(n\theta_l^*) \sin(s\theta_l^*) \cos(m\pi x_l^*/L) \cos(i\pi x_l^*/L) \right. \\ \left. + J_{x,l} \frac{n}{R} \frac{s}{R} \cos(n\theta_l^*) \cos(s\theta_l^*) \sin(m\pi x_l^*/L) \sin(i\pi x_l^*/L) \right\}. \quad (17)$$

The Rayleigh quotient for the problem studied is given by

$$\Omega^2 = \frac{V_S + V_{\tilde{k}} + V_c}{T_S^* + T_M^* + T_{MR}^*}, \quad (18)$$

$\Omega$  being the circular frequency (rad/s) of the system. The effect of fluid–structure interaction is added to Eq. (18) as shown by Amabili and Garziera (2000, 2002a, b). Only a finite number of modes in the Rayleigh–Ritz expansion are retained in numerical computations. The matrix  $\mathbf{q}$  of the Ritz coefficients is introduced,

$$q_{nmj} = \begin{cases} a_{nmj} & \text{for symmetric modes, } n = 0, \dots, N; \quad m = 1, \dots, \tilde{N}; \quad j = 1, 2, 3, \\ b_{nmj} & \text{for antisymmetric modes, } n = 1, \dots, N; \quad m = 1, \dots, \tilde{N}; \quad j = 1, 2, 3. \end{cases} \quad (19)$$

In Eq. (19) the expansion of symmetric and antisymmetric modes involves  $3 \times N \times \tilde{N}$  ( $3 \times (N+1) \times \tilde{N}$  for symmetric modes) terms;  $N$  and  $\tilde{N}$  must be chosen large enough to give the required accuracy.

The problem is solved minimizing the Rayleigh quotient, Eq. (18), which leads to the following Galerkin equation:

$$[\rho_S h(L/2) \mathbf{K}_S + \mathbf{K}_{\tilde{k}} + \mathbf{K}_c] \mathbf{q} - \Omega^2 [\rho_S h(L/2) \mathbf{M}_S + (M/R) (\mathbf{M}_M + \mathbf{M}_{MR})] \mathbf{q} = 0, \quad (20)$$

where matrices  $\mathbf{K}_S$ ,  $\mathbf{K}_{\tilde{k}}$ ,  $\mathbf{K}_c$ ,  $\mathbf{M}_S$ ,  $\mathbf{M}_M$  and  $\mathbf{M}_{MR}$  are easily obtained by the expression of potential and reference kinetic energies.

### 3. Numerical results

Calculations have been performed by using (i) the DIVA code (Amabili and Garziera, 2000, 2002a, b) modified to include rotary inertia, as described in Section 2; (ii) the commercial FEM program ANSYS. Numerical results have been carried out for a shell having the following dimensions and material properties:  $L = 0.52$  m,  $R = 0.1494$  m,  $h = 0.519$  mm,  $E = 198 \times 10^9$  Pa,  $\rho = 7850$  kg/m<sup>3</sup> and  $\nu = 0.3$ . The shell has been considered simply supported at the shell edges and four different configurations of added masses with rotary inertia have been considered. The first two cases are for one added mass (0.205 kg) at  $x_1 = L/4$  with small ( $90.36 \times 10^{-6}$  kg m<sup>2</sup>) and large ( $1.191 \times 10^{-3}$  kg m<sup>2</sup>) rotary inertia. Natural frequencies are presented in Tables 1 and 2, respectively. With respect to the case with neglected rotary inertia, two additional low-frequency modes appear. They are local modes because the movement is practically only rotation of the added mass. Except for these local modes, that require a huge number of terms in the Rayleigh–Ritz expansions used in the DIVA code in order to reach convergence, the agreement between DIVA and FEM results is quite good. In fact, the DIVA code, based on global discretization by using the Rayleigh–Ritz, is not efficient in describing very localized modes, which obviously require an extremely large number of terms in the Fourier expansions in order to be accurately described. Table 2 shows the convergence of DIVA code with the number of modes in the expansion, revealing that with  $N = 24$  and  $\tilde{N} = 44$  local modes are still far from convergence.

Table 1

Natural frequencies of the shell with one mass of  $M_1 = 0.205$  kg,  $J_{\theta,1} = J_{x,1} = 90.36 \times 10^{-6}$  kg m<sup>2</sup> placed at  $x_1 = L/4$ 

Mode	DIVA (Hz)	FEM (Hz)	Experiments (Hz)
1 A (local)	89.27	44.75	—
2 S (local)	121.23	50.08	—
3 S	131.52	127.29	152.7
4 A	215.86	214.15	—
5 S	220.17	219.96	217.2
6 A	232.89	230.28	—
7 S	241.99	241.17	240.6
8 A	264.97	263.91	—
9 S	272.95	272.51	269.6
10 A	287.98	285.23	—

Comparison of calculations with DIVA with  $N = 29$  and  $\tilde{N} = 49$ , commercial FEM code ANSYS and experiments (only symmetric modes). A = antisymmetric modes; S = symmetric modes.

Table 2

Natural frequencies of the shell with one mass of  $M_1 = 0.205$  kg,  $J_{\theta,1} = J_{x,1} = 1.191 \times 10^{-3}$  kg m<sup>2</sup> placed at  $x_1 = L/4$ 

Mode	DIVA, $N = 24$ , $\tilde{N} = 44$ (Hz)	DIVA, $N = 29$ , $\tilde{N} = 49$ (Hz)	FEM (Hz)	Experiments (Hz)
1 A (local)	27.05	24.83	12.33	—
2 S (local)	37.43	33.55	13.80	—
3 S	132.42	130.97	127.29	151.8
4 A	215.85	215.58	214.12	—
5 S	220.25	220.17	219.96	217.6
6 A	232.96	232.44	230.25	—
7 S	242.30	241.98	241.17	240.5
8 A	265.04	264.84	263.90	—
9 S	273.12	272.94	272.51	270.0
10 A	288.25	287.65	285.21	—

Comparison of calculations with DIVA, commercial FEM code ANSYS and experiments (only symmetric modes). A = antisymmetric modes; S = symmetric modes.

The other two cases studied are for two identical added masses (0.232 kg) at  $x_1 = x_2 = L/2$  (i.e. in the middle of the shell) and  $\theta_1 = 0.1396$  rad,  $\theta_2 = -0.1396$  rad, with medium ( $0.218 \times 10^{-3}$  kg m<sup>2</sup>) and large ( $2.26 \times 10^{-3}$  kg m<sup>2</sup>) rotary inertia. These two cases are different with respect to the previous ones, where symmetric modes were not affected by rotary inertia for symmetry reasons. In these two cases, reported in Tables 3 and 4, four additional local modes appear, due to the presence of two masses. Also in these cases, except for local modes, the agreement between DIVA and FEM results is quite good. The first eight mode shapes for the shell with two masses and large rotary inertia computed with DIVA are given in Appendix A and compared to experimental results.

The four cases numerically studied here correspond to the experiments reported in the next section.

Table 5 gives the natural frequencies of the shell with two identical added masses (0.232 kg) at  $x_1 = x_2 = L/2$  and  $\theta_1 = 0.1396$  rad,  $\theta_2 = -0.1396$  rad, with zero, medium ( $0.218 \times 10^{-3}$  kg m<sup>2</sup>) and large ( $2.26 \times 10^{-3}$  kg m<sup>2</sup>) rotary inertia. Excluding local modes, the case of zero rotary inertia presents the lowest natural frequency for each mode; the highest frequency is obtained for medium rotary inertia, which is slightly reduced for large rotary inertia. However, the maximum difference in frequency in the three cases is less than 5 Hz, giving around 4% of difference. It must be observed that, increasing the number of terms in the expansion used in the DIVA code, this difference in frequency decreases significantly.

A last case has been studied; it is the water-filled shell ( $\rho_F = 1000$  kg/m<sup>3</sup>) with two identical masses at  $x_1 = x_2 = L/2$  and  $\theta_1 = 0.1396$  rad,  $\theta_2 = -0.1396$  rad, with large ( $2.26 \times 10^{-3}$  kg m<sup>2</sup>) rotary inertia. Results are reported in Table 6 and

Table 3

Natural frequencies of the shell with two masses of  $M_1 = M_2 = 0.232$  kg,  $J_{\theta,1} = J_{\theta,2} = J_{x,1} = J_{x,2} = 0.218 \times 10^{-3}$  kg m<sup>2</sup> placed at  $x_1 = x_2 = L/2$  and  $\theta_1 = 0.1396$  rad,  $\theta_2 = -0.1396$  rad

Mode	DIVA (Hz)	FEM (Hz)	Experiments (Hz)
1 S (local)	57.37	27.01	—
2 A (local)	65.19	28.02	—
3 A (local)	86.20	31.27	—
4 S (local)	88.69	31.54	—
5 A	111.64	104.14	107.3
6 S	125.31	117.42	139.5
7 A	219.74	219.11	216.8
8 S	222.44	222.09	218.6
9 A	246.71	244.65	239.9
10 S	246.88	245.62	244.8
11 A	269.01	266.64	267.4
12 S	282.01	279.97	274.2

Comparison of calculations with DIVA with  $N = 24$  and  $\tilde{N} = 44$ , commercial FEM code ANSYS and experiments. A = antisymmetric modes; S = symmetric modes.

Table 4

Natural frequencies of the shell with two masses of  $M_1 = M_2 = 0.232$  kg,  $J_{\theta,1} = J_{\theta,2} = J_{x,1} = J_{x,2} = 2.26 \times 10^{-3}$  kg m<sup>2</sup> placed at  $x_1 = x_2 = L/2$  and  $\theta_1 = 0.1396$  rad,  $\theta_2 = -0.1396$  rad

Mode	DIVA (Hz)	FEM (Hz)	Experiments (Hz)
1 S (local)	18.03	8.60	—
2 A (local)	20.63	8.70	—
3 A (local)	26.78	9.71	—
4 S (local)	27.55	9.79	—
5 A	110.00	104.10	106.6
6 S	124.34	117.37	137.9
7 A	219.70	219.11	216.8
8 S	222.43	222.08	218.4
9 A	246.62	244.64	237.5
10 S	246.85	245.61	241.0
11 A	268.89	266.63	266.8
12 S	281.93	279.96	275.2

Comparison of calculations with DIVA with  $N = 24$  and  $\tilde{N} = 44$ , commercial FEM code ANSYS and experiments. A = antisymmetric modes; S = symmetric modes.

show that the contained water reduces significantly the natural frequencies; it also increases the modal mass, therefore reducing the effect of added masses.

#### 4. Experiments

Tests have been performed on a commercial circular cylindrical shell made of stainless steel and having a longitudinal seam weld. The dimensions and material properties of the shell are:  $L = 520$  mm,  $R = 149.4$  mm,  $h = 0.519$  mm,  $E = 1.98 \times 10^{11}$  Pa,  $\rho = 7850$  kg/m<sup>3</sup> and  $\nu = 0.3$ . Two stainless-steel annular plates of external and internal radius of 149.4 and 60 mm, respectively, and thickness 0.25 mm have been welded to the shell ends to approximate the simply supported boundary conditions of the shell. The shell has been suspended horizontally with cables to a box-type frame and it has been subjected to impact excitation in order to identify the natural frequencies and perform a modal analysis by measuring the shell response on a grid of points.

Table 5

Natural frequencies of the empty shell with two masses of  $M_1 = M_2 = 0.232$  kg placed at  $x_1 = x_2 = L/2$  and  $\theta_1 = 0.1396$  rad,  $\theta_2 = -0.1396$  rad, with  $J_{\theta,1} = J_{\theta,2} = J_{x,1} = J_{x,2} = J$

Mode	Frequency (Hz) without rotary inertia	Frequency (Hz) $J = 0.218 \times 10^{-3}$ kg m <sup>2</sup>	Frequency (Hz) $J = 2.26 \times 10^{-3}$ kg m <sup>2</sup>
1 S (local)	—	57.37	18.03
2 A (local)	—	65.19	20.63
3 A (local)	—	86.20	26.78
4 S (local)	—	88.69	27.55
5 A	106.77	111.64	110.00
6 S	120.43	125.31	124.34
7 A	219.22	219.74	219.70
8 S	222.21	222.44	222.43
9 A	245.23	246.71	246.62
10 S	246.18	246.88	246.85
11 A	266.81	269.01	268.89
12 S	279.72	282.01	281.93

Calculations with DIVA with  $N = 24$  and  $\tilde{N} = 44$ . A = antisymmetric modes; S = symmetric modes.

Table 6

Natural frequencies of the water-filled shell with two masses of  $M_1 = M_2 = 0.232$  kg placed at  $x_1 = x_2 = L/2$  and  $\theta_1 = 0.1396$  rad,  $\theta_2 = -0.1396$  rad, with and without rotary inertia of  $J_{\theta,1} = J_{\theta,2} = J_{x,1} = J_{x,2} = 2.26 \times 10^{-3}$  kg m<sup>2</sup>

Mode	Frequency (Hz) without rotary inertia	Frequency (Hz) with rotary inertia
1 S (local)	—	17.97
2 A (local)	—	20.53
3 A (local)	—	26.78
4 S (local)	—	27.55
5 S	71.82	73.93
6 A	72.18	75.89
7 A	82.47	84.53
8 S	82.63	83.35
9 A	86.80	86.80
10 S	87.21	88.09
11 A	107.56	107.77
12 S	112.42	114.38

Calculations with DIVA with  $N = 24$  and  $\tilde{N} = 44$ . A = antisymmetric modes; S = symmetric modes.

Four different cases, corresponding to the numerical calculations, have been considered. First two cases are for one mass (0.205 kg) at  $x_1 = L/4$  with small ( $90.36 \times 10^{-6}$  kg m<sup>2</sup>) and large ( $1.191 \times 10^{-3}$  kg m<sup>2</sup>) rotary inertia. The other two cases studied are for two identical masses (0.232 kg) at  $x_1 = x_2 = L/2$  (i.e. in the middle of the shell) and  $\theta_1 = 0.1396$  rad,  $\theta_2 = -0.1396$  rad, with medium ( $0.218 \times 10^{-3}$  kg m<sup>2</sup>) and large ( $2.26 \times 10^{-3}$  kg m<sup>2</sup>) rotary inertia. The experimental set-up for one of these cases is shown in Fig. 1.

The excitation has been provided by a miniature instrumented hammer B&K 8203. The shell response has been measured by using the accelerometer PCB 357A08 of 0.16 g. The time responses have been recorded by using the Difa Scadas II front-end connected to a HP c3000 workstation with the software CADA-X of LMS for signal processing and modal analysis. Frequency Response Functions (FRFs) have been estimated by using averages of eight measurements and the  $H_V$  algorithm.

Experimental results for the four cases are reported in Tables 1–4. The largest difference with respect to calculations is for mode 3 S in Tables 1 and 2. This is probably due to the finite dimension of the added mass (cylinder) used in the experiments (see Fig. 1); in the calculation this mass is considered of infinitesimal dimension. In Tables 1 and 2 only symmetric modes have been measured experimentally.



Fig. 1. Experimental shell with two masses with medium rotary inertia.

Table 7

Effect of rotary inertia on natural frequencies of the shell with two masses of  $M_1 = M_2 = 0.232$  kg,  $J_{\theta,1} = J_{\theta,2} = J_{x,1} = J_{x,2} = J$  placed at  $x_1 = x_2 = L/2$  and  $\theta_1 = 0.1396$  rad,  $\theta_2 = -0.1396$  rad experimentally measured

Mode	$J = 0.218 \times 10^{-3} \text{ kg m}^2$	$J = 2.26 \times 10^{-3} \text{ kg m}^2$
5 A	107.3	106.6
6 S	139.5	137.9
7 A	216.8	216.8
8 S	218.6	218.4
9 A	239.9	237.5
10 S	244.8	241.0
11 A	267.4	266.8
12 S	274.2	275.2

A = antisymmetric modes; S = symmetric modes.

Table 7 shows a comparison of experimental natural frequencies (excluding local modes, that have not been identified in the modal analysis) of the shell with two masses for the two cases of different rotary inertia. Results show that the increase of rotary inertia generally reduces natural frequencies but by an extremely small quantity; only modes 5 A and 6 S, which are the ones largely affected by the two added masses (also if rotary inertia is neglected), present a larger reduction of the order of 1%. Similar reduction is predicted by DIVA, while FEM results show an even smaller effect.

## 5. Conclusions

The computer code DIVA has been successfully modified to include the effect of rotary inertia of added masses. This has been done in order to satisfy an industrial application. Results show that the effect of rotary inertia on shells is negligible in the cases studied [this is in contrast with what has been found for thin plates (Amabili et al., 2005), due to the geometric stiffness of the circular cylindrical shell], except for two additional local modes, due to the rotational degrees of freedom, for each mass with rotary inertia. These local modes have low frequency and they can be practically excited only by the rotation of the added masses; in fact, these modes have not been detected by the experimental modal analysis performed. These modes can be more conveniently calculated by using a FEM code than by using the



Rayleigh–Ritz approach of DIVA for their local characteristics; in fact, the Rayleigh–Ritz method is based on global discretization and in order to capture local modes a very high number of modes in the expansion must be used.

**Acknowledgements**

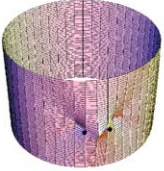
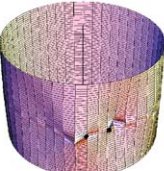

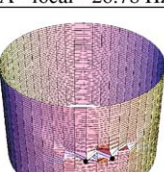
This work was partially supported by the FIRB 2001 and COFIN 2003 grants of the Italian Ministry for University and Research (MIUR). Ing. F. Boccia, F. Magnani, S. Sabaini and Dr M. Pellegrini are thanked for helping the authors in the experiments and data processing.

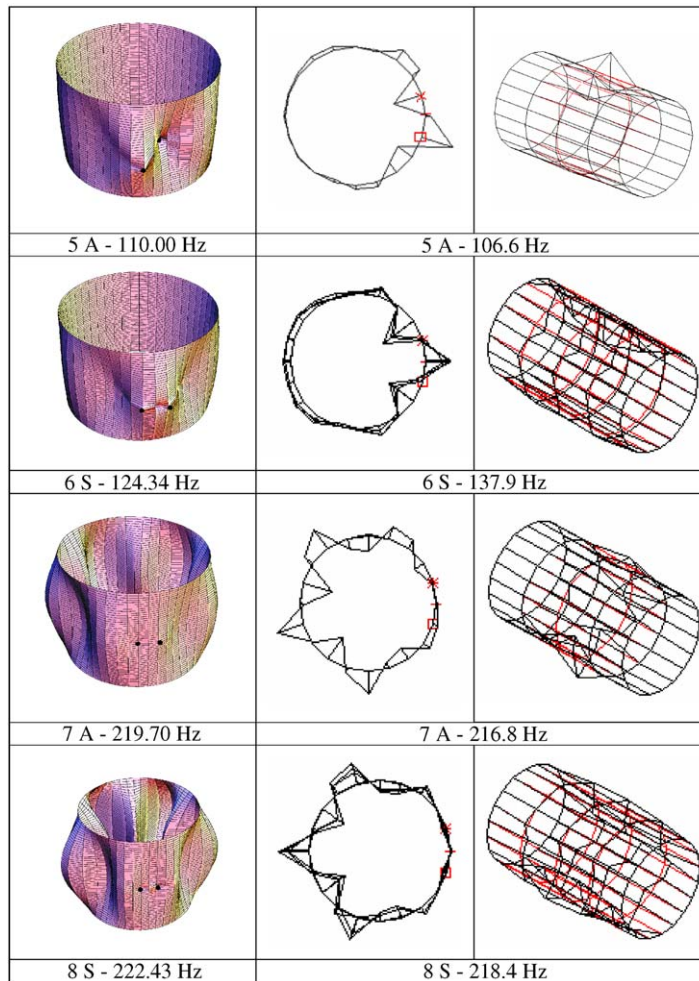
**Appendix A. Mode shapes**

The mode shapes for various modes of the shell, some compared with experiment, are given in Table A1.

Table A1

Comparison of computed (DIVA,  $N = 24$ ,  $\tilde{N} = 44$ ) and experimentally identified mode shapes of the shell with two masses of  $M_1 = M_2 = 0.232 \text{ kg}$  placed at  $x_1 = x_2 = L/2$  and  $\theta_1 = 0.1396 \text{ rad}$ ,  $\theta_2 = -0.1396 \text{ rad}$ , with rotary inertia of  $J_{\theta,1} = J_{\theta,2} = J_{x,1} = J_{x,2} = 2.26 \times 10^{-3} \text{ kg m}^2$

DIVA	Experiments	
	N.A.	N.A.
1 S - local - 18.03 Hz		
	N.A.	N.A.
2 A - local - 20.63 Hz		
	N.A.	N.A.
3 A - local - 26.78 Hz		
	N.A.	N.A.
4 S - local - 27.55 Hz		



A = antisymmetric modes; S = symmetric modes; N.A. = not available in experiments; ●, X, □ = location of masses.

## References

- Amabili, M., 1996. Free vibration of a fluid-filled circular cylindrical shell with lumped masses attached, using the receptance method. *Shock Vib.* 3, 159–167.
- Amabili, M., Garziera, R., 1999. A technique for the systematic choice of admissible functions in the Rayleigh–Ritz method. *J. Sound Vib.* 224, 519–539.
- Amabili, M., Garziera, R., 2000. Vibrations of circular cylindrical shells with nonuniform constraints, elastic bed and added mass; Part I: empty and fluid-filled shells. *J. Fluids Struct.* 14, 669–690.
- Amabili, M., Garziera, R., 2002a. Vibrations of circular cylindrical shells with nonuniform constraints, elastic bed and added mass; Part II: shells containing or immersed in axial flow. *J. Fluids Struct.* 16, 31–51.
- Amabili, M., Garziera, R., 2002b. Vibrations of circular cylindrical shells with nonuniform constraints, elastic bed and added mass; Part III: steady viscous effects on shells conveying fluid. *J. Fluids Struct.* 16, 795–809.
- Amabili, M., Pellegrini, M., Righi, F., Vinci, F., 2005. Effect of concentrated masses with rotary inertia on vibrations of rectangular plates. *Journal of Sound and Vibration*, submitted for publication.
- Leissa, A.W., 1973. *Vibration of Shells*, NASA SP-288. Government Printing Office, Washington, DC Now available from The Acoustical Society of America (1993).
- Soedel, W., 1993. *Vibrations of Shells and Plates*, second ed. Marcel Dekker, New York.